Exciton emission in PTCDA films and PTCDA/Alq_3 multilayers

H. P. Wagner and A. DeSilva
Department of Physics, University of Cincinnati, Cincinnati, Ohio 45221-0011, USA

T. U. Kampen
Department of Molecular Physics, Fritz-Haber-Institut der Max-Planck-Gesellschaft, 14195 Berlin, Germany
(Received 17 June 2004; revised manuscript received 16 September 2004; published 1 December 2004)

We investigate the exciton emission in 3,4,9,10-perylene tetracarboxylic dianhydride (PTCDA) thin films and PTCDA/aluminium-tris-hydroxyqinoline (Alq_3) multilayers by photoluminescence spectroscopy in the temperature range from 10 to 300 K. The films are grown by organic molecular beam deposition on Si(001) and Pyrex™ substrates at high vacuum. The obtained temperature dependence of the different recombination channels arising from indirect Frenkel excitons, charge transfer excitons, excimers, and relaxed excited monomers is compared to the recombination channels in single PTCDA crystals. A strong recombination band is observed at 1.63 eV in PTCDA/Alq_3 multilayers. This emission band is attributed to charge transfer transitions between stacked PTCDA molecules that are compressed by strain fields within the PTCDA layers. This assignment is supported by strain-dependent photoluminescence measurements on pure PTCDA films.

DOI: 10.1103/PhysRevB.70.235201 PACS number(s): 78.55.Kz, 78.20.Bh, 78.47.+p, 71.35.Aa

I. INTRODUCTION

Thin films of organic semiconductors based on π-conjugated molecules have attracted enormous interest because of various applications such as organic light-emitting diodes (OLEDs),[1–5] demonstrations of solar cells,[6,7] and field-effect transistors.[8] However, despite recent improvements in device performance, the microscopic understanding of recombination processes in organic crystals and films is still rather limited.

One of the most intensively used molecules to study the influence of intermolecular interactions on the structural, optical, and electronic properties in organic crystals is 3,4,9,10,- perylene tetracarboxylic dianhydride (PTCDA), which crystallizes in the monoclinic space group C_{2h} with two nearly coplanar molecules in the unit cell.[9,10] Two different crystalline modifications, α- and β-phase, are known.[11–14] For both phases, the molecules in a PTCDA crystal form stacks that are parallel to the a-direction in the crystal, which is the direction of growth of needle-like PTCDA crystallites. The equal orientation of molecules within all stacks results in a layered structure, with the molecules being parallel to the (102) plane with their long symmetry axis. Along the long symmetry axis, the molecules are tilted by 11° with respect to the (102) plane.[15,16] In thin films grown on substrates like Ag(111),[17] Au(111),[18] and highly oriented pyrolitic graphite,[19] PTCDA is adsorbed in a "herringbone" structure, with two molecules in each unit cell almost perpendicular to each other and parallel to the substrate surface. This arrangement of the molecules is similar to the one in the (102) plane of a PTCDA crystal. The tendency of PTCDA to form well ordered thin films makes it a promising material for the fabrication of organic multilayers with abrupt interfaces.

The optical bandgap of PTCDA thin films is defined by the first absorption peak at 2.22 eV,[20] which is due to the highest occupied molecular orbital (HOMO) to lowest unoccupied molecular orbital (LUMO) excitation which couples to several molecular vibrations. The most strongly coupled modes are almost degenerate and can be replaced by a single internal effective mode, thus simplifying theoretical calculations. Recently, a theoretical model of various recombination processes in α-PTCDA single crystals was developed,[21,22] which is based on time-resolved photoluminescence (PL) measurements that were performed in a temperature range between 10 and 300 K. From the various recombination times that were detected within the emission band, six different exciton emission channels could be isolated: A high-energy emission band due to a relaxed monomer transition, a pronounced indirect Frenkel exciton transition, two different charge transfer transitions, and an excimer transition that becomes the dominant band at higher temperatures.

Despite the progress in thin-film growth techniques (e.g., the organic molecular-beam deposition (OMBD)[9,23] or the organic vapor-phase deposition[24,25]) many fewer systematic photoluminescence investigations have been performed on crystalline PTCDA films or PTCDA containing organic multilayer structures so far.[8,25–29] An interesting organic molecule for multilayer investigations is tris (8-hydroxy) quinoline aluminum (Alq_3) that has attracted much attention as a superior material for OLEDs.[1,3] Alq_3 serves as the electron transporting layer and is responsible for the emission of light. PTCDA has been shown to serve as an efficient hole injection layer in OLED structures.[30,31] To produce low-cost matrix displays, OLEDs with transparent top electrodes have to be prepared. This is achieved by inverting the OLED structure; i.e., depositing an indium tin oxide (ITO) anode by sputter deposition onto the organic films. PTCDA has been shown to withstand sputter deposition of ITO with minimal degradation in its conducting properties,[32] showing the potential of PTCDA in such inverted structures.

In contrast to planar PTCDA molecules that result in highly ordered polycrystalline layers, the propeller shaped Alq_3 molecules in general form amorphous films.[33,34] It is therefore of importance to investigate how the crystalline structure of PTCDA films that are embedded in Alq_3 layers

changes compared to pure PTCDA films. In particular, different exciton emission channels can be strongly affected by structural changes and generated strain fields within the PTCDA layer. In addition, HOMO-LUMO offset measurements using photoelectron spectroscopy[35] indicate an intermolecular charge transfer transition (at 1.85 eV) at the PTCDA/Alq_3 interface. Such multilayer structures may be used to modify the optical constants and the emission spectrum in organic devices.

In the present work we investigate the exciton emission in OMBD-grown crystalline PTCDA films and PTCDA/Alq_3 multilayers by temperature-dependent PL spectroscopy. Since our investigations are focused on intrinsic film properties, the films are prepared on weakly interacting substrates like Si with natural oxide surface or Pyrex™. The observed emission bands from films and multilayers are compared to recombination channels obtained from single PTCDA crystals.[21,22] The PL and absorption measurements are accompanied by structural investigations using x-ray diffraction and far infrared Fourier transform (FTIR) absorption measurements.

II. EXPERIMENTAL DETAILS

The investigated PTCDA and Alq_3 films as well as PTCDA/Alq_3 multilayers were grown by OMBD at room temperature on chemically clean *n*-type (001) oriented Si (resistivity: $1-5\ \Omega\,\mathrm{cm}$) and on amorphous Pyrex™ substrates. The substrates were cleaned in an ultrasonic bath using acetone, methanol, and ultrapure water. They were then transferred into the high vacuum OMBD chamber with a base pressure of 10^{-8} mbar. The PTCDA and Alq_3 source materials (Sigma Aldrich) were purified by sublimation under high vacuum (10^{-6} mbar) at temperatures of 300 and 210 °C, respectively, before they were filled into the Knudsen cells. During growth, the deposition rate was measured using a quartz crystal thickness monitor that was calibrated by different film thickness measurements using a profilometer, optical ellipsometry, and absorption measurements. Typical deposition rates from the effusion cells are 0.01 nm/s at temperatures of 320 and 230 °C for the PTCDA and Alq_3, respectively. Computer controlled mechanical shutters at the Knudsen cells enable a nanometer thickness control of PTCDA films and organic PTCDA/Alq_3 multilayers.

A 50 W tungsten halogen lamp was used as light source for transmission measurements of films and multilayers on Pyrex™ substrates. In the PL measurements, the films were either excited by frequency doubled 100 fs Ti/sapphire laser pulses at 2.84 eV ($\lambda = 436$ nm) or by a cw solid-state laser at 2.33 eV ($\lambda = 532$ nm). To avoid any structural damage in the organic films, the average laser power was set below 0.1 mW in all PL measurements. The absorption and PL spectra were analyzed by a grating monochromator and a GaAs photomultiplier. The spectral response of the entire detection system was determined with blackbody radiation using a tungsten halogen lamp with given emission spectra. Because of the flatness of the spectral response in the PTCDA emission range (1.5 to 2.2 eV) no spectral correction was applied to the PL measurements. For variable temperature measurements between 10 and 300 K, a closed-cycle He cryostat (CTI-Cryogenics) was used. For strain-dependent PL measurements, the PTCDA film on Si substrate was placed into a uniaxial pressure cell where a metal piston is pressing the sample against a sapphire window.

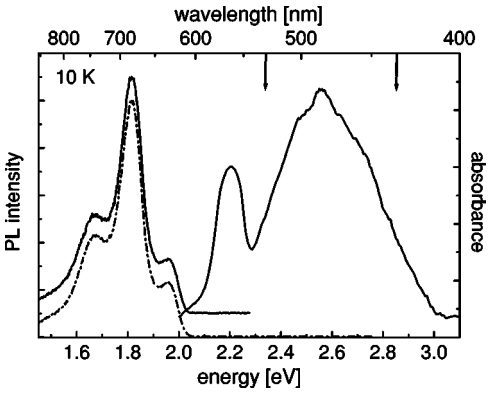

FIG. 1. PL spectra of a 36 nm thick PTCDA film on Si(001) excited at two different excitation energies (2.33 and 2.84 eV) indicated as vertical arrows and absorption spectrum of a 70 nm thick PTCDA film on Pyrex™ recorded at 10 K. The spectra are offset for better comparison.

X-ray diffraction patterns of the PTCDA films and PTCDA/Alq_3 multilayers were collected using a Rigaku DMAX-2000 diffractometer with Cu K_{α_1} radiation. The data were recorded in θ-2θ scan mode at room temperature.

III. EXPERIMENTAL RESULTS AND DISCUSSION

A. PTCDA thin films

Figure 1 shows the PL spectra at 10 K of a 36 nm thick PTCDA film grown on Si (001) for two different excitation energies (2.84 and 2.33 eV) as indicated by vertical arrows. In addition, the absorption spectrum of a 70 nm PTCDA film on Pyrex™ is displayed revealing a narrow absorption band at 2.22 eV that is attributed to a zero-vibron π-π^* Frenkel exciton transition.[36] This 0-0 absorption line is followed by a broad and slightly structured band centered at 2.53 eV, which is attributed to Frenkel exciton transitions into higher vibronic subbands. A more detailed investigation on temperature-dependent absorption in PTCDA films[37] as well as a discussion about other absorption models will be given elsewhere.[38,39] For a better comparison, the two PL spectra and the absorption spectrum are slightly offset to each other. No significant changes in the PL spectrum are observed as the excitation energy is changed from 2.84 eV on the high-energy side of the π-π^* absorption to 2.33 eV closer to the narrow 0-0 exciton absorption band. Compared to the PL obtained from single PTCDA crystals,[21,22] the PTCDA film shows a very similar PL structure; however, the whole emission is shifted to lower energies by approximately 20 meV. A possible explanation for this redshift might be different strain within the film[40] and in the single crystals. Furthermore, the PTCDA film reveals a more pronounced high-energy band at 1.95 eV compared to the PTCDA crystals. From energetic reasons, this band cannot be attributed to a

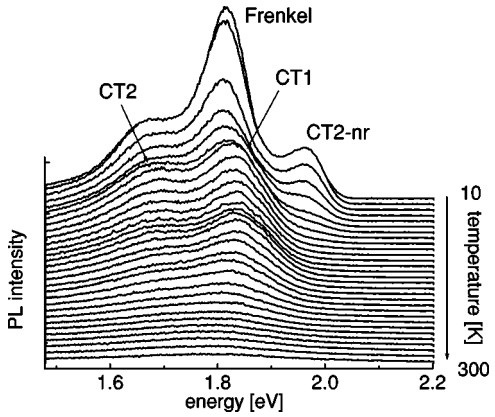

FIG. 2. Temperature-dependent PL of a 36 nm thick PTCDA film on Si(001) excited at 2.84 eV in the range 10 to 300 K in 10 K steps. The contributing emission channels are labeled.

relaxed monomer transition. Recent calculations[41,42] show that this transition might be assigned to a nonrelaxed charge transfer exciton transition between stacked molecules in different unit cells, denoted as CT2-nr in what follows. Figure 2 demonstrates temperature-dependent PL spectra of the same PTCDA film in 10 K steps. Again, the PL of the PTCDA film shows a temperature dependence similar to that observed in single crystals.[21,22] With increasing temperature the high-energy CT2-nr band and the dominating Frenkel exciton emission strongly decrease. Above 50 K the relaxed charge transfer transitions CT1 between molecules within the same unit cell and relaxed CT2 between stacked molecules in different unit cells become the dominating emission bands. Their temperature decrease is weaker compared to the CT2-nr and the Frenkel exciton luminescence.

A more detailed analysis of these bands is shown in Fig. 3 for 20, 80, and 300 K, where we applied model calculations

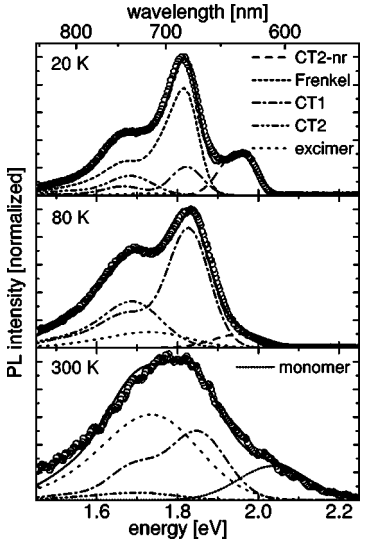

FIG. 3. PL spectra of a 36 nm thick PTCDA film on Si(001) excited at 2.33 eV obtained at temperatures 20, 80, and 300 K. The experimental data is shown as open circles. Also shown are results of model calculations. The individual emission channels are labeled, the resulting calculated PL spectrum is shown as a solid line.

that were developed for PTCDA single crystals. The asymmetric Frenkel exciton emission, including vibronic progressions of external and internal vibrational modes, is reconstructed by six normalized Gaussian functions:[21]

$$I_{\mathrm{PL}}(\hbar\omega) = \omega^3 \sum_j \frac{a_j}{\sigma_j\sqrt{2\pi}} \exp\left[-\frac{1}{2}\left(\frac{\omega-\omega_j}{\sigma_j}\right)^2\right]. \qquad (1)$$

Compared to the PL investigations on bulk PTCDA crystals, the peak energies $\hbar\omega_j$ of the Gaussian lines in PTCDA films have been shifted by 26 meV to lower energies, while the full widths at half-maxima (FWHM) $\sqrt{8\ln 2}\hbar\sigma_j$ as well as the areas of the Gaussian functions a_j were not changed. The temperature dependence of the Gaussian broadening σ_j was considered using the relation[22]

$$\sigma_j^2 = \sigma_{0j}^2 + \alpha_{\mathrm{int}}^2(\hbar\omega_{\mathrm{int}})^2 \coth\left(\frac{\hbar\omega_{\mathrm{int}}}{2k_BT}\right) + \alpha_{\mathrm{ext}}^2(\hbar\omega_{\mathrm{ext}})^2 \coth\left(\frac{\hbar\omega_{\mathrm{ext}}}{2k_BT}\right), \qquad (2)$$

where the different FWHM of the Gaussian functions σ_{0j} are given by 69, 92, 104, 123, and 158 meV.[16] The values of the reorganization energy and frequency of internal modes $\alpha_{\mathrm{int}}^2 = 0.29$, $\omega_{\mathrm{int}} = 233\ \mathrm{cm}^{-1}$ were taken from Refs. 22 and 43 and values of the external modes $\alpha_{\mathrm{ext}}^2 = 7.5$ and $\omega_{\mathrm{ext}} = 50\ \mathrm{cm}^{-1}$ were taken from Refs. 27 and 44. The parameters used for the Frenkel exciton emission are summarized in Table I.

Each of the PL bands related to self-trapped excitons (CT1, CT2, and excimer) is modeled as a sum of normalized Gaussians with positions ω_j, broadenings σ_j, and areas a_j, as given in Eq. (1). However, the spacing between subsequent positions ω_j now corresponds to one effective vibrational mode energy $\hbar\omega_{\mathrm{eff}} \approx 160$ meV, and the ratio of the areas a_j of the vibronic subbands are described according to Poisson distributions.[22] As for the Frenkel exciton emission, the Gaussian center energies $\hbar\omega_j$ have been shifted to lower energies by 26 meV, while the other parameters σ_j and a_j were kept the same as for the PTCDA single crystals. The temperature-dependent broadenings $\sigma_j(T)$ for the self-trapped excitons are free fitting parameters that allow one to interpolate the PL line shape between different temperatures. Due to thermal expansion and an increased occupation of higher vibrational subbands, all bands shift to higher energies with rising temperature, except for the excimer transition, which shows no noticeable temperature shift. In our calculations we used the same blueshifts for the Frenkel exciton and CT2 emission as given in Ref. 4, but we doubled the blueshift of the CT1 emission in order to achieve a better fitting with the experimental data. Finally, the high-energy CT2-nr transition and an additional weak high-energy band that occurs at high temperatures and is attributed to a relaxed monomer transition were considered by a single Gaussian function with transition energies $\hbar\omega_j = 1.944$ and 2.05 eV. The broadenings were set to $\sqrt{8\ln 2}\hbar\sigma_j = 100$ meV for both lines. A blueshift of 6×10^{-2} meV/K is introduced to the 1.944 eV band. All parameters used for the self-trapped exciton emissions and high-energy transitions are summarized in Table I.

TABLE I. Model parameters for all six emission channels. For each Gaussian function, the peak energies $\hbar\omega_j$ in the limit $T=\rightarrow 0$ K, the FWHM $\sqrt{8\ln 2}\hbar\sigma_j$, its relative area a_j, and temperature blueshift are given.

Emission channels	j	Peak energy [eV]	FWHM [meV]	Area	Blueshift [meV/K]
Frenkel exciton	1	1.824	69	0.494	4.8×10^{-2}
	2	1.774	92	0.506	
	3	1.674	104	0.336	
	4	1.604	123	0.183	
	5	1.504	158	0.150	
CT1	1	1.819	92	1.000	7.8×10^{-2}
	2	1.661	118	0.530	
	3	1.503	164	0.140	
CT2	1	1.679	128	1.000	6.2×10^{-2}
	2	1.525	160	0.400	
Excimer	1	1.731	140	1.000	0
	2	1.586	160	0.460	
CT2-nr	1	1.944	100	1.000	6.0×10^{-2}
Monomer	1	2.05	100	1.000	0

The agreement between the experimental results obtained from the PTCDA thin film and the model calculations that are based on earlier investigations on PTCDA crystals are very good demonstrating the high structural and optical quality of our PTCDA films. The good structural quality is also supported by x-ray measurements depicted in Fig. 4(a), which show a completely symmetric α-PTCDA (102) reflex with an α/β-PTCDA ratio of better 40:1 and a FWHM of 0.37° for the α-PTCDA reflex occurring at $2\theta=27.81°$.

B. PTCDA/Alq_3 multilayers

Figure 5 shows the PL spectra of a PTCDA/Alq_3 multilayer structure grown on Si(001) comprising six alternating PTCDA and Alq_3 layers of 3 and 4 nm thickness, respectively. The two PL spectra were recorded at 10 K at different excitation energies (2.84 eV and 2.33 eV), as indicated by vertical arrows. The absorption spectrum of the multilayer on Pyrex™ is also shown. In comparison to the absorption spectrum on pure PTCDA films the absorption above 2.6 eV is slightly enhanced due to the onset of the Alq_3 absorption in these films. Correspondingly, the PL spectrum excited at 2.84 eV shows the Alq_3 emission[45,46] peaking at 2.37 eV. The Alq_3 emission is absent when the multilayer is excited at 2.33 eV where Alq_3 is transparent. Besides the appearance of the Alq_3 luminescence the PTCDA emission is not affected by changing the laser excitation energies. As for the PTCDA thin film, the PL spectra and the absorption curve are offset to each other for better

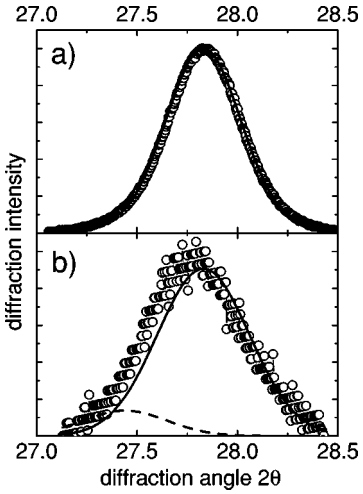

FIG. 4. X-ray diffraction spectra (a) on a 70 nm thick PTCDA film and (b) on a $6\times$[PTCDA 3 nm/Alq_3 4 nm] multilayer. Both structures were grown on Si(001). The solid and dashed lines show Gaussian fits for α- and β-PTCDA (102) reflexes, respectively.

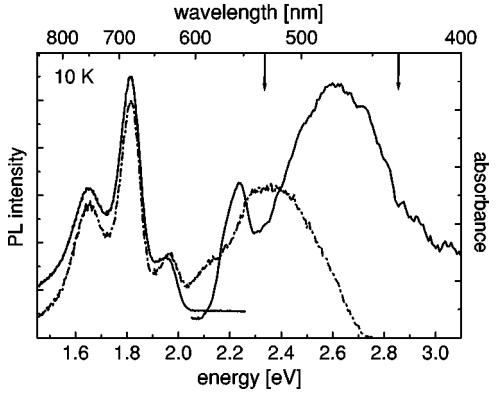

FIG. 5. PL spectra of a $6\times$[PTCDA 3 nm/Alq_3 4 nm] multilayer grown on Si(001) excited at two different excitation energies (2.33 and 2.84 eV) indicated as vertical arrows and absorption spectrum of the same multilayer grown on Pyrex™ recorded at 10 K. The spectra are offset for better comparison.

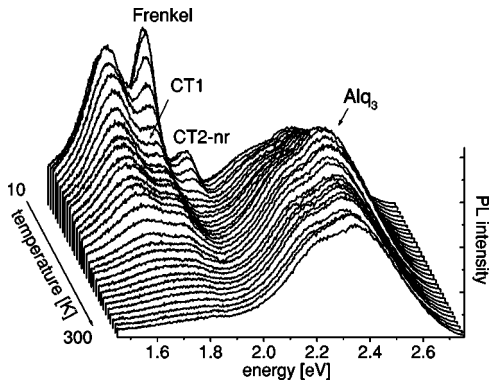

FIG. 6. Temperature-dependent PL of a $6\times$[PTCDA 3 nm/Alq_3 4 nm] multilayer on Si(001) excited at 2.84 eV in the range 10 to 300 K in 10 K steps. The contributing emission channels are labeled.

comparison. While the CT2-nr and Frenkel exciton emission lines are not energetically shifted and also have similar PL intensities as compared to the PTCDA film, a closer look at the low-energy emission shows a more pronounced and red-shifted band. This observation becomes more obvious in temperature-dependent PL measurements (excited at 2.84 eV) as demonstrated in Fig. 6. Above 40 K the low-energy peak becomes the governing emission and remains dominant up to 200 K. (The temperature dependence of the Alq_3 emission is treated in a forthcoming publication.[47]) As for the PTCDA film, we applied model calculations on the PTCDA/Alq_3 multilayers for 20, 80 and 300 K (see Fig. 7), where we kept the parameters given in Table I. To achieve a satisfying agreement of the simulated data with the experimental data an additional Gaussian line at $\hbar\omega_j = 1.63$ eV, with a FWHM of 100 meV and a blueshift of 4.0

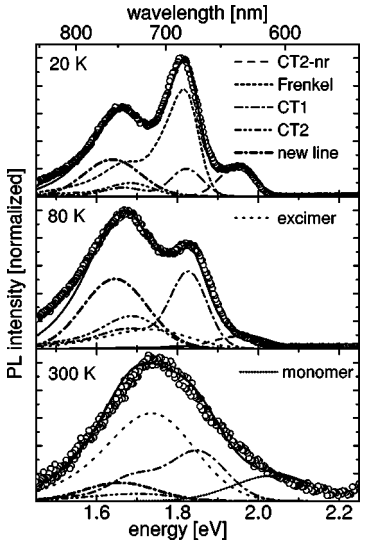

FIG. 7. PL spectra of a $6\times$[PTCDA 3 nm/Alq_3 4 nm] multilayer on Si(001) excited at 2.33 eV obtained at temperatures 20, 80, and 300 K. The experimental data are shown as open circles. Also shown are results of model calculations. The individual emission channels are labeled; the resulting calculated PL spectrum is shown as a solid line.

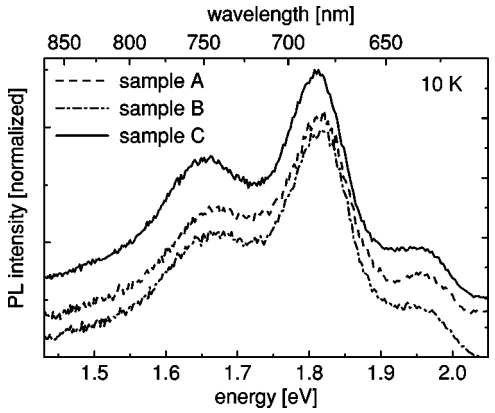

FIG. 8. Normalized PL spectra of a 10 nm PTCDA film on Si(001) (sample A), a 10 nm PTCDA film on a 2 nm Alq_3 layer on Si (001) (sample B), and a 2 nm Alq_3 layer on a 10 nm PTCDA film on Si (001) (sample C) excited at 2.84 eV and recorded at 10 K. The spectra are offset for better comparison.

$\times 10^{-2}$ meV/K had to be introduced. While the relative weight of the CT2 emission channel is suppressed by the introduction of the new line, the relative ratios and the overall temperature dependence of the Frenkel exciton and self-trapped exciton emission bands are very similar compared to the pure PTCDA film.

The appearance of the new channel in the PTCDA/Alq_3 multilayers can have different reasons: The low-energy emission could be due to an interface transition at the multilayer interface as indicated by x-ray photoelectron spectroscopy measurements.[35] Alternatively, the emission could be due to the reabsorption of the Alq_3 emission at the lowest PTCDA absorption subband according to observations of a low-energy *Y*-band, where a PTCDA film was excited at 2.2 eV.[27,28] Furthermore, the low-energy emission could be explained by structural changes and strain effects within the crystalline PTCDA layers that are grown on amorphous Alq_3 layers.

To decide which one of the above explanations is appropriate, we performed additional PL measurements on three different samples that were grown on Si (001). The first sample (A) is a pure PTCDA film of 10 nm thickness, the second (B) is a 10 nm PTCDA thin film with a 2 nm thick Alq_3 layer on top, and the third (C) is a 10 nm thick PTCDA film which was grown on a 2 nm thick Alq_3 layer. The obtained normalized PL spectra performed at 10 K are shown in Fig. 8. While there is no difference in the emission from samples A and B we obtain a clear appearance of a new line in sample C. As observed in the multilayer structures, this new line becomes the dominant emission band above 40 K (not shown here), while the temperature dependence of sample B is equal to the pure PTCDA film (sample A). Since we have introduced a PTCDA/Alq_3 interface in samples B and C, a PTCDA/Alq_3 interface transition cannot be the reason for the low-energy emission line. Furthermore, since reabsorption from the Alq_3 film occurs in samples B and C, this process is also not responsible for the occurrence of the low-energy emission. Therefore, we conclude that structural changes within the PTCDA films are the microscopic origins for the appearance of the new emission band at 1.63 eV.

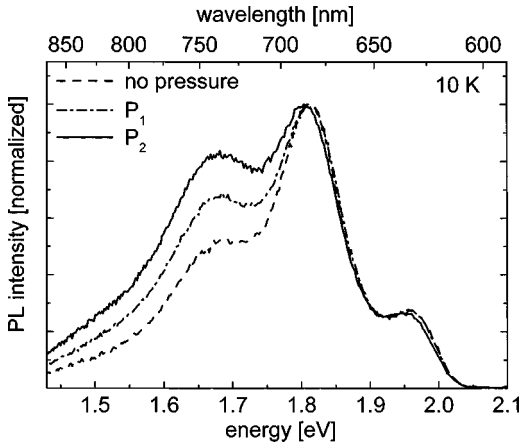

FIG. 9. Normalized PL spectra of a 36 nm PTCDA film on Si (001) without and with applied uniaxial strains P_1 and P_2. ($P_2 > P_1$) The layer was excited at 2.33 eV and the spectra were recorded at 10 K.

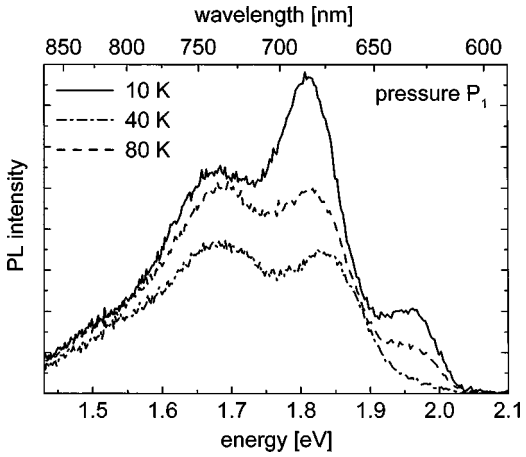

FIG. 10. Temperature-dependent PL spectra of a 36 nm PTCDA film on Si(001) with applied uniaxial strain. The layer was excited at 2.33 eV and the spectra were recorded at 10, 40, and 80 K.

For a more specific explanation of this structural change, we performed x-ray diffraction measurements on the multilayer samples [see Fig. 4(b)]. They show an α/β-PTCDA ratio of 8:1 and reveal a significant broader FWHM of 0.46° for the α-PTCDA (102) reflex. The broader FWHM reflex indicates inhomogeneous strain inside the PTCDA crystallites within the multilayer structure. In addition, far infrared absorption measurements performed with a Fourier spectrometer show slightly more pronounced out-of-plane vibrational modes at 733 and 809 cm^{-1} in PTCDA/Alq_3 multilayers than in pure PTCDA films,[47] indicating tilted PTCDA crystallites.[48]

In agreement to observations of Ref. 30, we conclude that the crystalline α-phase is essentially not changed when the PTCDA is embedded in Alq_3. The individual PTCDA crystals, however, are tilted with respect to the growth direction. This tilt causes strain fields within the PTCDA film, where a compressive component along the π-orbitals of stacked molecules significantly affects transition CT2. Due to the reduced distance between the stacked molecules the CT exciton binding energy and the CT exciton formation probability are increased causing a more pronounced emission line in the PL spectrum. Correspondingly, the new emission line is attributed to a strain-modified CT2 emission band with strong asymmetric line shape due to the strain dependence of the emission intensity. This interpretation also explains why the fitting procedure using a weak "old" CT2 Gaussian line and a strong "new" CT2 line led to a better agreement than the use of one single redshifted Gaussian function that does not address the strong asymmetry of the strain-modified emission band.

For further support of our interpretation, we performed strain-dependent PL measurements on a 36 nm thick PTCDA film at 10 K using a pressure cell that produces a uniaxial strain up to about 1 kbar along the film growth direction. The applied strain has been estimated from PL experiments on sublimed PTCDA single crystals using a cryogenic diamond-anvil cell.[49] As demonstrated in Fig. 9, the low-energy CT2 emission slightly shifts to lower energy and increases its intensity when uniaxial strain P_1 (about 0.5 kbar) and higher strain P_2 (about 1 kbar) is applied to the PTCDA film. The weaker redshift of the CT2 emission compared to the emission in PTCDA/Alq_3 multilayers is attributed to strain inhomogeneities and missing in-plane strain components in these measurements. Finally, Fig. 10 shows the PL spectra of the 32 nm PTCDA film at 20, 40, and 80 K that were recorded at strain P_1. As in the PTCDA/Alq_3 multilayers, the low-energy emission gains intensity relative to the Frenkel exciton emission when the temperature is raised and becomes the dominating band above 40 K, confirming our interpretation of a strain-modified CT2 emission.

IV. SUMMARY

We studied the exciton emission in PTCDA thin films and PTCDA/Alq_3 multilayers performing temperature-dependent PL measurements. The different recombination channels arising from Frenkel excitons, charge transfer excitons (CT1-nr, CT1, CT2), excimers, and relaxed excited monomers that were observed earlier in PTCDA single crystals also appear in PTCDA thin films and in PTCDA/Alq_3 multilayers in a very similar way. However, in PTCDA/Alq_3 multilayers an unknown low-energy line dominates the emission spectrum up to 200 K. This low-energy line appears if the PTCDA film is grown on Alq_3 while it disappears when Alq_3 is grown on PTCDA, demonstrating that the low-energy line is not generated by the PTCDA/Alq_3 interface transition. Investigations of the structural properties of PTCDA films and multilayers using x-ray diffraction and FTIR absorption reveal an increase of out-of-plane disorder of PTCDA molecules in the multilayer structure. This observation indicates the presence of tilted PTCDA crystallites within the multilayer structure causing strain fields that affect the CT2 transition between stacked PTCDA molecules. Uniaxial strain-dependent PL measurements on pure PTCDA films identify the dominating low-energy band observed in PTCDA/Alq_3 multilayers as a strain-modified charge-transfer exciton transition CT2.

ACKNOWLEDGMENTS

The authors acknowledge Dr. Boolchand and Dr. Ahn for performing x-ray diffraction measurements and supporting the profilometer and ellipsometry measurements, respectively. We thank Dr. Kim for carrying out FTIR absorption measurements on PTCDA and multilayer samples. The experimental support of H. Schmitzer and H. P. Tranitz is kindly acknowledged. The authors are also indebted to Dr. Scholz and Dr. Weinstein for fruitful discussions.

[1] C. W. Tang and S. A. VanSlyke, Appl. Phys. Lett. **51**, 913 (1987).
[2] M. A. Baldo, D. F. O'Brien, Y. You, A. Shoustikov, S. Sibley, M. E. Thompson, and S. R. Forrest, Nature (London) **395**, 151 (1998).
[3] R. H. Friend *et al.*, Nature (London) **397**, 121 (1999).
[4] M. A. Baldo, M. E. Thompson, and S. R. Forrest, Nature (London) **403**, 750 (2000).
[5] J. Huang, M. Pfeiffer, A. Werner, J. Blochwitz, S. Liu, and K. Leo, Appl. Phys. Lett. **80**, 139 (2002).
[6] P. Peumans, V. Bulovic, and S. R. Forrest, Appl. Phys. Lett. **76**, 2650 (2000).
[7] D. Meissner and J. Rostalski, Synth. Met. **121**, 1551 (2001).
[8] R. Hajlaoui, G. Horowitz, F. Garnier, A. Arce-Brouchet, K. Laigre, A. El Kassimi, F. Demanze, and K. Kouki, Adv. Mater. (Weinheim, Ger.) **9**, 389 (1997).
[9] S. R. Forrest, Chem. Rev. (Washington, D.C.) **97**, 1793 (1997).
[10] A. J. Lovinger, S. R. Forrest, M. L. Kaplan, P. H. Schmidt, and T. Venkatesan, J. Appl. Phys. **55**, 476 (1984).
[11] A. Aziz and L. L. Narasimhan, Synth. Met. **131**, 71 (2002).
[12] B. Krause, A. C. Dürr, K. Ritley, F. Schreiber, H. Dosch, and D. Smilgies, Phys. Rev. B **66**, 235404 (2002).
[13] A. J. Lovinger, S. R. Forrest, M. L. Kaplan, P. H. Schmidt, and T. Venkatesan, Bull. Am. Phys. Soc. **28**, 363 (1983).
[14] M. L. Kaplan, C. S. Day, A. J. Lovinger, and P. H. Schmidt (private communication).
[15] I. Chizhov, A. Kahn, and G. Scoles, J. Cryst. Growth **208**, 449 (2000).
[16] T. Ogawa, K. Kuwamotot, S. Isoda, T. Kobayashi, and N. Karl, Acta Crystallogr., Sect. B: Struct. Sci. **B55**, 123 (1999).
[17] E. Umbach, K. Glöckner, and M. Sokolowski, Surf. Sci. **402–404**, 20 (1998).
[18] T. Schmitz-Hübsch, T. Fritz, F. Sellam, R. Straub, and K. Leo, Phys. Rev. B **55**, 7972 (1997).
[19] C. Kendrick, A. Kahn, and S. R. Forrest, Appl. Surf. Sci. **104/105**, 586 (1996).
[20] R. Kaiser, M. Friedrich, T. Schmitz-Hübsch, F. Sellam, T. U. Kampen, K. Leo, and D. R. T. Zahn, Fresenius' J. Anal. Chem. **363**, 189 (1999).
[21] A. Yu. Kobitski, R. Scholz, I. Vragović, H. P. Wagner, and D. R. T. Zahn, Phys. Rev. B **66**, 153204 (2002).
[22] A. Yu. Kobitski, R. Scholz, D. R. T. Zahn, and H. P. Wagner, Phys. Rev. B **68**, 155201 (2003).
[23] H. Fuchigami, S. Tanimura, Y. Uehara, T. Kurata, and S. Tsunoda, Jpn. J. Appl. Phys., Part 2 **34**, 3852 (1995).
[24] M. A. Baldo, V. G. Kozlov, P. E. Burrows, S. R. Forrest, V. S. Ban, B. Koene, and M. E. Thompson, Appl. Phys. Lett. **71**, 3033 (1997).
[25] M. Shtein, H. F. Gossenberger, J. B. Benzinger, and S. R. Forrest, J. Appl. Phys. **89**, 1470 (2001).
[26] A. Yu. Kobitski, R. Scholz, G. Salvan, T. U. Kampen, H. P. Wagner, and D. R. T. Zahn, Appl. Surf. Sci. **212–213**, 428 (2003).
[27] U. Gómez, M. Leonhardt, H. Port, and H. C. Wolf, Chem. Phys. Lett. **268**, 1 (1997).
[28] M. Leonhardt, O. Mager, and H. Port, Chem. Phys. Lett. **313**, 24 (1999).
[29] S. Heutz, A. J. Ferguson, G. Rumbles, and T. S. Jones, Org. Electron. **3**, 119 (2002).
[30] E. Burrows and S. R. Forrest, Appl. Phys. Lett. **64**, 2285 (1994).
[31] V. Bulović, P. E. Burrows, S. R. Forrest, J. A. Cronin, and M. E. Thompson, Chem. Phys. **210**, 13 (1996).
[32] F. So and S. R. Forrest, IEEE Trans. Electron Devices **36**, 66 (1989).
[33] S. Heutz and T. S. Jones, J. Appl. Phys. **92**, 3030 (2002).
[34] S. Tohito, J. Sakata, and Y. Taga, Appl. Phys. Lett. **64**, 1353 (1999).
[35] I. G. Hill, D. Milliron, J. Schwartz, and A. Kahn, Appl. Surf. Sci. **166**, 354 (2000).
[36] I. Vragovic, R. Scholz, and M. Schreiber, Europhys. Lett. **57**, 288 (2002).
[37] H. P. Wagner, V. Ganglienka, A. DeSilva, and R. Scholz (unpublished).
[38] I. Vragovic and R. Scholz, Phys. Rev. B **68**, 155202 (2003).
[39] M. Hoffmann and Z. G. Soos, Phys. Rev. B **66**, 024305 (2002).
[40] P. Fenter, F. Schreber, L. Zhou, P. Eisenberger, and S. R. Forrest, Phys. Rev. B **56**, 3046 (1997).
[41] R. Scholz, A. Yu. Kobitski, I. Vragovic, T. U. Kampen, D. R. T. Zahn, and H. P. Wagner, Inst. Phys. Conf. Ser. **171**, 266 (2002).
[42] R. Scholz (unpublished).
[43] R. Scholz, A. Yu. Kobitski, T. U. Kampen, M. Schreiber, D. R. T. Zahn, G. Jungnickel, M. Sternberg, and Th. Frauenheim, Phys. Rev. B **61**, 13 659 (2000).
[44] V. Bulović, P. E. Burrows, S. R. Forrest, J. A. Cronin, and M. E. Thompson, Chem. Phys. **210**, 1 (1996).
[45] A. B. Djurišić, C. Y. Kwong, T. W. Lau, E. H. Li, Z. T. Liu, H. S. Kwok, L. S. M. Lam, and W. K. Chan, Appl. Phys. A: Mater. Sci. Process. **76**, 219 (2003).
[46] A. Aziz and L. L. Narasimhan, Synth. Met. **131**, 71 (2002).
[47] H. P. Wagner and A. DeSilva (unpublished).
[48] R. Scholz, M. Friedrich, G. Salvan, T. U. Kampen, D. T. R. Zahn, and T. Frauenheim, J. Phys.: Condens. Matter **15**, 2647 (2003).
[49] R. E. Tallman, B. A. Weinstein, A. DeSilva, and H. P. Wagner, Phys. Status Solidi C (to be published).